AXL is associated with STAT3 activation in breast cancer

GUOAN ZHANG[1,2*], XIAOBAI SUN[3*], JUNPING ZHANG[4], ZHAOZHEN ZHANG[1,2], XINLIN LUAN[1,2], FENGYUAN YU[1,2], ZHENJIE GUAN[1,2], CHANGMING GUO[1,2], YANGYANG HU[1,2], MENGFEI ZHAO[1,2], JIARONG E.[1,2], YINGXIN XIONG[1,2], JUNZE LIU[1,2], YUQING HU[5], XINYU MA[5], RUIYAO YANG[5], JIANLI LIU[6], HONGLI ZHAO[7] and QINGWEI GUO[8]

[1]School of Forensic Medicine, Jining Medical University, Jining, Shandong 272067, P.R. China; [2]Jining Key Laboratory of Forensic Multimodal Precision Identification, Jining, Shandong 272067, P.R. China; [3]Department of Medical Technology, Jinan Vocational College of Nursing, Jinan, Shandong 250102, P.R. China; [4]Department of Pathology, Liangshan People's Hospital, Jining, Shandong 272600, P.R. China; [5]School of Mental Health (Research Institute of Mental Health), Jining Medical University, Jining, Shandong 272067, P.R. China; [6]Department of Pathology, Affiliated Hospital of Jining Medical University, Jining, Shandong 272029, P.R. China; [7]Department of Gastroenterology, Digestive Diseases Hospital of Shandong First Medical University, Jining, Shandong 272067, P.R. China; [8]Department of Hematology and Oncology, and Department of Child Health, Jinan Children's Hospital, Jinan, Shandong 250022, P.R. China

Received February 5, 2026; Accepted July 31, 2026

DOI: 10.3892/mco.2026.2969

Abstract. Breast cancer (BC) represents one of the most frequently occurring malignancies and a primary cause of cancer-associated mortality among women globally. AXL, a receptor tyrosine kinase of the TAM family, and signal transducer and activator of transcription 3 (STAT3) are both aberrantly activated in BC and contribute to tumor progression. The present study aimed to investigate the functional association between AXL and STAT3 activation in BC. It was found that the overexpression of AXL in MCF7 and 293T cells enhanced STAT3 phosphorylation and transcriptional activity, whereas AXL knockdown using short hairpin RNA or pharmacological inhibition with R428 suppressed STAT3 activation. AXL overexpression also enhanced the secretion of IL-6, a major upstream activator of STAT3. Bioinformatics analysis of clinical BC datasets (GSE102484, GSE9893 and The Cancer Proteome Atlas) validated a positive correlation between AXL expression and STAT3 signaling activation. Collectively, these findings demonstrate that AXL is associated with STAT3 activation in BC, providing insight into the molecular pathways driving BC progression and uncovering candidate therapeutic targets.

Correspondence to: Dr Qingwei Guo, Department of Hematology and Oncology, and Department of Child Health, Jinan Children's Hospital, 23976 Jingshi Road, Jinan, Shandong 250022, P.R. China
E-mail: gqw2007@163.com

Dr Hongli Zhao, Department of Gastroenterology, Digestive Diseases Hospital of Shandong First Medical University, 11 Taibailou Middle Road, Jining, Shandong 272067, P.R. China
E-mail: xushulinfeng@163.com

*Contributed equally

Key words: AXL, signal transducer and activator of transcription 3, breast cancer

Introduction

Breast cancer (BC) is the most common malignancy affecting women worldwide, with diverse molecular subtypes and complex pathogenic mechanisms (1-3). In 2022, it was estimated that there were >2 million new BC cases worldwide, accounting for 11.6% of all cancer cases. A subset of BCs, known as triple-negative BC (TNBC), lacks the expression of estrogen receptor (ER), progesterone receptor (PR) and HER2, and accounts for ~10-20% of all BC cases. TNBC often belongs to the basal-like molecular subtype. These tumors are aggressive with a poor prognosis due to ineffective target therapies. Therefore, identifying key signaling pathways driving BC progression is crucial for developing effective therapeutic strategies (4,5).

AXL is a receptor tyrosine kinase of the TAM (Tyro3, AXL, Mer) family, activated upon binding its ligand growth arrest-specific 6 (Gas6) (6-9). AXL is frequently overexpressed in BC, particularly TNBC, and promotes epithelial-to-mesenchymal transition and metastasis and is associated with a poor prognosis by activating multiple downstream signaling pathways, including phosphoinositide 3-kinase (PI3K) and AKT (protein kinase B), as well as mitogen-activated protein kinase and extracellular signal-regulated kinase (ERK) (10-15).

Signal transducer and activator of transcription 3 (STAT3) is a critical transcription factor that mediates signaling from cytokines (for example, IL-6) and growth factors (16,17). The aberrant activation of STAT3, primarily via tyrosine-705 phosphorylation, is a common oncogenic event in BC (18). Activated STAT3 dimerizes and translocates to the nucleus to regulate

the transcription of genes governing cell cycle progression, anti-apoptosis and metastasis. The IL-6/JAK/STAT3 signaling axis is well-documented as a driver of BC progression and drug resistance (19,20).

Emerging evidence suggests a crosstalk between AXL and STAT3 signaling in multiple cancer types. A previous study by the authors revealed an association between AXL and STAT3 activation in esophageal squamous cell carcinoma by Gene Set Enrichment Analysis (GSEA) analysis (21). Khera *et al* (22) reported that the activation of AXL by GAS6 induced the phosphorylation of proline-rich tyrosine kinase 2, a non-receptor tyrosine kinase that serves as an essential upstream mediator of STAT3 activation. In a previous study on gastric cancer, co-culture with cancer-associated fibroblasts (CAFs) triggered STAT3 activation, which was reversed by the AXL inhibitor, 9im, although the selectivity of 9im requires further validation (23). Similarly, Hung *et al* (24) demonstrated that AXL signaling within lung cancer cells and CAF directly drives the secretion of IL-11, which binds to the GP130 complex and activates STAT3 in tumor-associated macrophages (TAMs). Concordant AXL-STAT3 signaling polarizes TAMs toward an M2-like phenotype, upregulates CD44 and mesenchymal markers, and enhances macrophage-mediated vasculogenic network formation. The dual inhibition of AXL and STAT3 disrupts this paracrine loop, reduces TAM recruitment and polarization, and suppresses tumor growth in lung cancer xenograft models (24). However, the direct functional link between AXL and STAT3 activation in BC remains poorly defined.

Thus, it was hypothesized that AXL modulates STAT3 activation in BC cells. Using *in vitro* experiments and clinical dataset analyses, the present study aimed to validate this hypothesis and to establish a functional association between AXL and STAT3 signaling in BC.

Materials and methods

Cell lines and reagents. MCF7 (cat. no. SCSP-531), 293T (cat. no. SCSP-502), MDA-MB-231 (cat. no. SCSP-5043) and HeLa (cat. no. SCSP-504) cells were purchased from The Cell Bank of Type Culture Collection of the Chinese Academy of Sciences. MCF7 cells were cultured in MEM (Procell Life Science & Technology, Co., Ltd.) supplemented with 0.01 mg/ml insulin and 10% fetal bovine serum (FBS). The 293T, MDA-MB-231 and HeLa cells were maintained in DMEM (Gibco; Thermo Fisher Scientific, Inc.) containing 10% FBS. All cells were incubated at 37˚C in a humidified atmosphere with 5% CO_2. Cell line authentication was performed by short tandem repeat profiling at the Forensic Science Center, Jining Medical University. IL-6 was purchased from PeproTech, Inc. R428 and tocilizumab were obtained from MedChemExpress. R428 was used as previously described (25), and tocilizumab was used at 25 μg/ml.

Plasmids, short hairpin RNA (shRNA) and transfection. AXL plasmid (cat. no. 105932, based on pcDNA4/TO/myc/HIS) was obtained from Addgene, Inc. The STAT3 reporter plasmid (SIE vector) and pRL-TK vector were purchased from Promega Corporation. Lentivirus for shRNA targeting AXL (shAXL: 5'-GGGTGACAATGTGGGAGATTG-3') and control shRNA (Ctrl: 5'-TTCTCCGACGTGTCACGT-3') were purchased from Shanghai GenePharma Co., Ltd. as pre-packaged, ready-to-use viral particles (3rd-generation, packaged in 293T cells; titer 10^9 TU/ml). Transfection of plasmids (1 μg for one well of 12-well plate) was performed using Lipo8000 (Beyotime Institute of Biotechnology) according to the manufacturer's protocol. Briefly, Lipo8000 and plasmids were incubated in DMEM without FBS for 5 min and added the cell medium for 4 h at 37˚C. A total of 44-48 h later, cells were harvested for analysis. For lentiviral transfection, viruses (5 μl/ml) and polybrene (2 μg/ml) were added to the cell medium at MOI=5, incubated at 37˚C/5% CO_2 for 16 h before medium change. After 3 days cells were treated with puromycin (2 μg/ml) for 1 week to select transfected cells. Then, cells were cultured at puromycin (0.5 μg/ml) for maintenance. These stable cell lines were used for experiments.

Nuclear and cytoplasmic protein extraction. Nuclear and cytoplasmic proteins were extracted using a nuclear and cytoplasmic protein extraction kit (cat. no. P0027; Beyotime Institute of Biotechnology) according to the manufacturer's instructions. These experiments were repeated three times.

Western blot analysis. Western blot analysis was performed as previously reported (25,26). Total cellular proteins were extracted using RIPA buffer supplemented with protease and phosphatase inhibitors sourced from Beyotime Institute of Biotechnology. Subsequently, nuclear and cytoplasmic proteins were isolated using a dedicated nuclear-cytoplasmic protein extraction kit (Beyotime Institute of Biotechnology). The protein concentration was precisely measured using the BCA Protein Assay kit (Beyotime Institute of Biotechnology). Equal quantities (10 μg) of these proteins were resolved through 10% SDS-PAGE and then transferred to PVDF membranes. The membranes were first blocked for 1 h at room temperature in a 5% non-fat milk solution. They were then incubated overnight at 4˚C with an array of primary antibodies: AXL (1:1,000; cat. no. 8661), phosphorylated (p)-AKT (1:1,000; cat. no. 4060), STAT3 (1:1,000; cat. no. 9139), Histone H3 (1:1,000; cat. no. 9715), p-STAT3 (1:1,000; cat. no. 9145), AKT (1:1,000; cat. no. 4691; Cell Signaling Technology, Inc.), ERK1 + ERK2 (1:10,000; cat. no. ab184699), p-ERK1 + ERK2 (1:10,000; cat. no. ab76299) (all from Abcam), GAPDH antibody (1:1,000; cat. no. 60004-1-Ig; Proteintech Group, Inc.) and p-AXL (1:200; cat. no. AF2228; R&D Systems, Inc.). Post-incubation with the primary antibodies, the membranes were further incubated with peroxidase-conjugated goat anti-rabbit (cat. no. ZB-2301) or goat anti-mouse (cat. no. ZB-2305) secondary antibodies, both from OriGene Technologies Inc., at a dilution of 1:5,000 for 1 h at room temperature. Immunoreactive bands were detected using ECL reagent from Beyotime Institute of Biotechnology. GAPDH and histone H3 were employed as loading controls for cytoplasmic and nuclear proteins, respectively. All the experiments were repeated at least three times. ImageJ software (version 1.53m; National Institutes of Health) was used for the densitometric analysis.

Dual luciferase reporter gene assay. Cells underwent co-transfection with an SIE vector serving as a STAT3 reporter, a pRL-TK vector acting as an internal control,

and either an empty vector (EV) or an AXL plasmid using Lipo8000 (Beyotime Institute of Biotechnology) according to the manufacturer's protocol. For each well of a 12-well plate, a total of 1 μg plasmid DNA was transfected, comprising 0.5 μg AXL plasmid (or empty vector), 0.45 μg STAT3 reporter plasmid (SIE vector), and 0.05 μg pRL-TK internal control plasmid. The transfection complexes were incubated with cells for 4 h at 37˚C in a humidified incubator with 5% CO_2, after which the medium was replaced with fresh complete medium carefully. At 48 h post-transfection, luciferase activity was determined by employing the Dual Luciferase Reporter Gene Assay kit from Beyotime Institute of Biotechnology (cat. no. RG029M), strictly adhering to the manufacturer's guidelines. In the inhibitor experiments, cells were transfected with 0.45 μg STAT3 reporter plasmid (SIE vector), and 0.05 μg pRL-TK internal control plasmid. 24 h later, the cells were incubated with R428 at a concentration of 1, 3 μM or DMSO for another 24 h followed by luciferase activity determination. This experiment was repeated three times with triplicate wells for each condition, and data was normalized by comparison with *Renilla* luciferase activity.

Reverse transcription-quantitative PCR (RT-qPCR). Total RNA was extracted using TRIzol reagent (Invitrogen; Thermo Fisher Scientific, Inc.). First-strand cDNA was synthesized using PrimeScript RT Master Mix (Takara Biotechnology, Co., Ltd.) according to the manufacturer's instructions. qPCR was performed using SYBR-Green PCR Master Mix (Vazyme Biotech Co., Ltd.) on a QuantStudio 5 Real-Time PCR system (Thermo Fisher Scientific, Inc.). Each qPCR reaction was performed in a final volume of 20 μl, containing 10 μl SYBR Green Master mix (2X), 0.5 μl forward and reverse primers (10 μM), 8 μl DEPC treated water and 1 μl cDNA. The following thermocycling conditions were used for the qPCR: 95˚C for 30 sec, 40 cycles of 95˚C for 10 sec and 60˚C for 30 sec. The primer sequences for IL-6 and 18S were as follows: IL-6 forward, 5'-CACAGACAGCCACTCACCTC-3' (sense) and reverse, 5'-TTTTCTGCCAGTGCCTCTTT-3' (antisense); 18S rRNA, 5'-GAGGATGAGGTGGAACGT GT-3' (sense) and reverse, 5'-GGACCTGGCTGTATTTTC CA-3' (antisense). 18S was used as an internal control. Relative gene expression was calculated using the $2^{-\Delta\Delta Cq}$ method (27). This experiment was repeated three times with triplicate wells for each condition.

ELISA. The IL-6 concentration in the cell culture supernatants was measured using an IL-6 ELISA kit [cat. no. EK106; Hangzhou Multi Sciences (Lianke) Biotech Co., Ltd.] according to the manufacturer's protocol. This experiment was repeated three times with triplicate wells for each condition.

Bioinformatics analysis. Gene expression datasets GSE102484 (n=683) (28) and GSE9893 (n=155) (29) were downloaded from the Gene Expression Omnibus database (https://www.ncbi.nlm.nih.gov/geo/). GSEA was performed to compare IL6_JAK_STAT3 signaling between the AXL-high and AXL-low groups as reported in a previous study by the authors (21). Protein expression data of AXL and p-STAT3 (Y705) from breast invasive carcinoma were obtained from The Cancer Proteome Atlas (TCPA, n=901) (https://www.tcpaportal.org/tcpa/download.html); the samples whose AXL expression marked with NA (n=156) were excluded. The association between the expression of AXL and p-STAT3 was analyzed with SPSS (version 13.0; SPSS, Inc.) using Pearson's correlation analysis (n=745). The association analysis between AXL mRNA and IL-6 mRNA in BC was performed by gepia2 using Pearson's correlation analysis as the method to calculate the correlation coefficient (http://gepia2.cancer-pku.cn/#correlation) (30).

Statistical analysis. Data are presented as the mean ± standard deviation (SD). Differences between two groups were analyzed using a two-tailed unpaired Student's t-test. Comparisons among multiple groups were performed by one-way analysis of variance (ANOVA) followed by Dunnett's post hoc test using GraphPad Prism 8 (GraphPad Software, Inc.; Dotmatics). $P<0.05$ was considered to indicate a statistically significant difference.

Results

AXL overexpression enhances STAT3 activation in BC cells. To investigate the effects of AXL on STAT3 activation, AXL was overexpressed in MCF7 and 293T cells. Western blot analysis revealed that AXL overexpression significantly increased p-STAT3 (Y705) levels without altering total STAT3 (t-STAT3) expression (Fig. 1A and B). Moreover, AXL overexpression enhanced p-STAT3 (Y705) levels in both cell lines in a concentration-dependent manner (0, 1 and 2 μg) (Fig. 1C and D).

Subcellular fractionation analysis revealed that AXL overexpression increased nuclear STAT3 levels in MCF7 cells, indicating an enhanced STAT3 nuclear translocation (Fig. 1E). A port of AXL was also detected in the nucleus, consistent with a previous study (31). Dual luciferase reporter assay confirmed that AXL overexpression significantly augmented STAT3 transcriptional activity in MCF7 and 293T cells (Fig. 1F and G). Additionally, AXL overexpression upregulated IL-6 mRNA expression and secretion, as measured using RT-qPCR and ELISA, respectively (Fig. 1H and I). Furthermore, GEPIA2 analysis further validated an association between AXL and IL-6 mRNA in clinical BC samples ($P=4.1x10^{-7}$) (Fig. 1J). Treatment with the IL-6 receptor-neutralizing antibody, tocilizumab, partly abrogated the AXL-induced activation of STAT3 (Fig. 1K). These results suggest that AXL activates STAT3, at least in part by promoting IL-6 secretion.

AXL suppression inhibits STAT3 activation. To further confirm the role of AXL in STAT3 activation, AXL was knocked down in MDA-MB-231 and HeLa cells, which express high endogenous AXL. The results of western blot analysis demonstrated that the shRNA-mediated AXL knockdown significantly reduced STAT3 activation (Fig. 2A and B). Pharmacological inhibition with the selective AXL inhibitor, R428, also decreased AXL and STAT3 activation in the MDA-MB-231 cells in a concentration-dependent manner (Fig. 2C and D). Furthermore, R428 treatment dose reduced STAT3 transcriptional activity in a concentration-dependent manner (Fig. 2E).

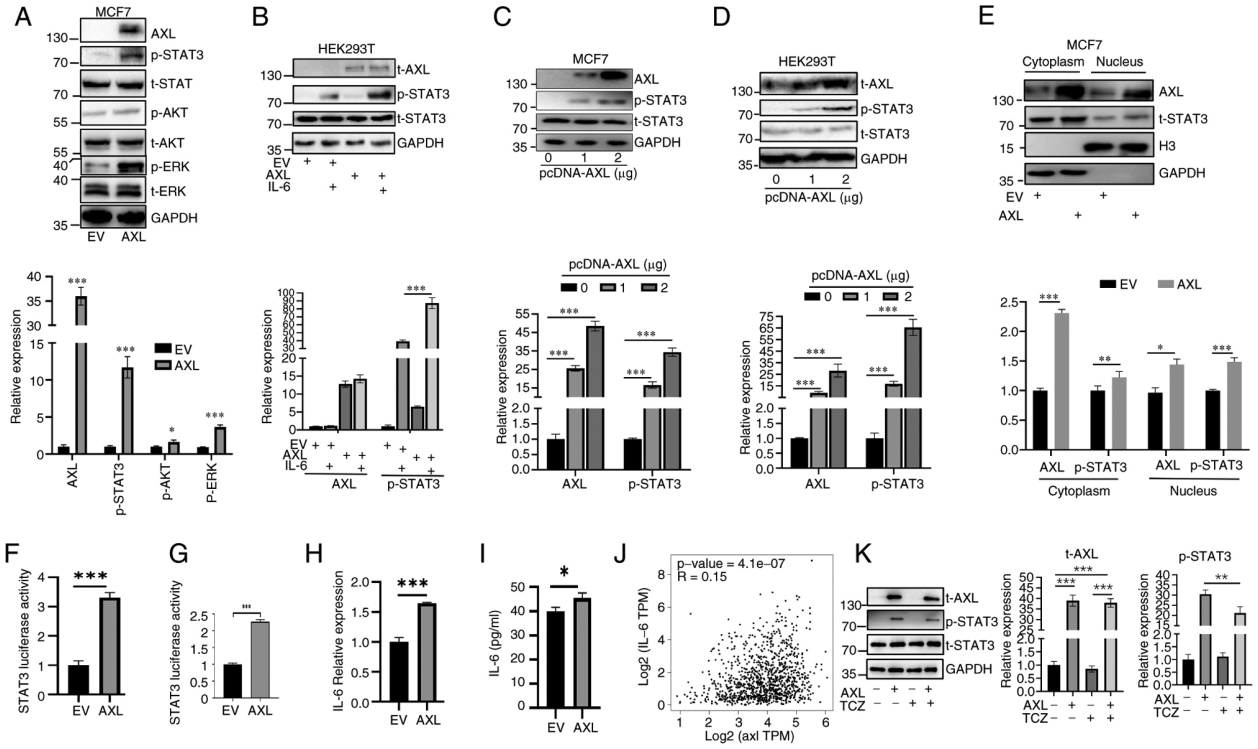

Figure 1. AXL overexpression enhances STAT3 activation. (A) MCF7 cells were transfected with empty plasmid (EV) or AXL plasmid; the indicated proteins were examined using western blot analysis. (B) 293T cells were transfected with empty plasmid (EV) or AXL plasmid for 24 h and treated with or without IL-6 (10 ng/ml) for 30 min; the indicated proteins were examined using western blot analysis. (C) MCF7 cells were transfected with increasing amounts of AXL plasmid for 48 h and the indicated proteins were examined using western blot analysis. (D) 293T cells were transfected with increasing amounts of AXL plasmid for 48 h and the indicated proteins were examined using western blot analysis. (E) MCF7 cells transfected with empty plasmid (EV) or AXL plasmid; the indicated proteins were examined using western blot analysis. (F) MCF7 cells were co-transfected with empty plasmid (EV) or AXL plasmid, as well as STAT3 reporter plasmid (SIE vector) and pRL-TK vector for 48 h and analyzed using the Dual Luciferase Reporter Gene Assay kit. (G) 293T cells were co-transfected with empty plasmid (EV) or AXL plasmid, as well as STAT3 reporter plasmid (SIE vector) and pRL-TK vector for 48 h and analyzed using the Dual Luciferase Reporter Gene Assay kit. (H) MCF7 cells transfected with empty plasmid (EV) or AXL plasmid; the mRNA expression of IL-6 was determined using reverse transcription-quantitative PCR. (I) MCF7 cells transfected with empty plasmid (EV) or AXL plasmid; IL-6 levels in the cell supernatants was determined using ELISA. (J) Scatter plot illustrating the correlation between the mRNA expression levels of AXL and IL-6 analyzed using the GEPIA2 online tool. (K) MCF7 cells were transfected with EV (-) or AXL plasmid (+) for 48 h and then treated with or without tocilizimab (25 μg/ml) for 24 h. The indicated proteins were examined using western blot analysis. t-, total. *P<0.05, **P<0.01 and ***P<0.001. EV, empty vector; p-, phosphorylated.

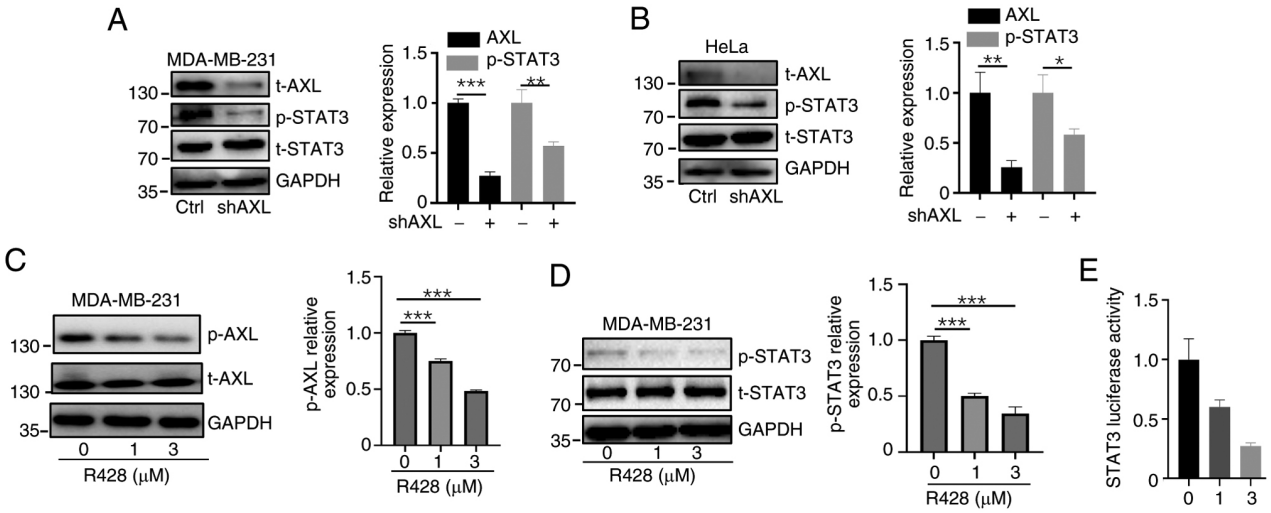

Figure 2. AXL suppression decreases STAT3 activation. (A) MDA-MB-231 cells were transfected with AXL-shRNA lentivirus (shAXL) or control lentivirus (Ctrl) for 48 h and treated with puromycin (2 μg/ml) for ~1 week to select transfected cells. The indicated proteins were examined using western blot analysis. (B) HeLa cells were transfected with AXL-shRNA lentivirus (shAXL) or control lentivirus (Ctrl) for 48 h and treated with puromycin (2 μg/ml) for ~1 week to select transfected cells. The indicated proteins were examined using western blot analysis. (C and D) MDA-MB-231 cells were treated with increasing concentration of R428 for 24 h. The indicated proteins were examined using western blot analysis. (E) MDA-MB-231 cells were co-transfected with empty plasmid (EV) or AXL plasmid, as well as STAT3 reporter plasmid (SIE vector) and pRL-TK vector for 24 h and treated with DMSO (Ctrl) or R428 (1 and 3 μM) for a further 24 h; STAT3 activity was analyzed using the Dual Luciferase Reporter Gene Assay kit. *P<0.05, **P<0.01, ***P<0.001. shRNA, short-hairpin RNA; EV, empty vector; p-, phosphorylated.

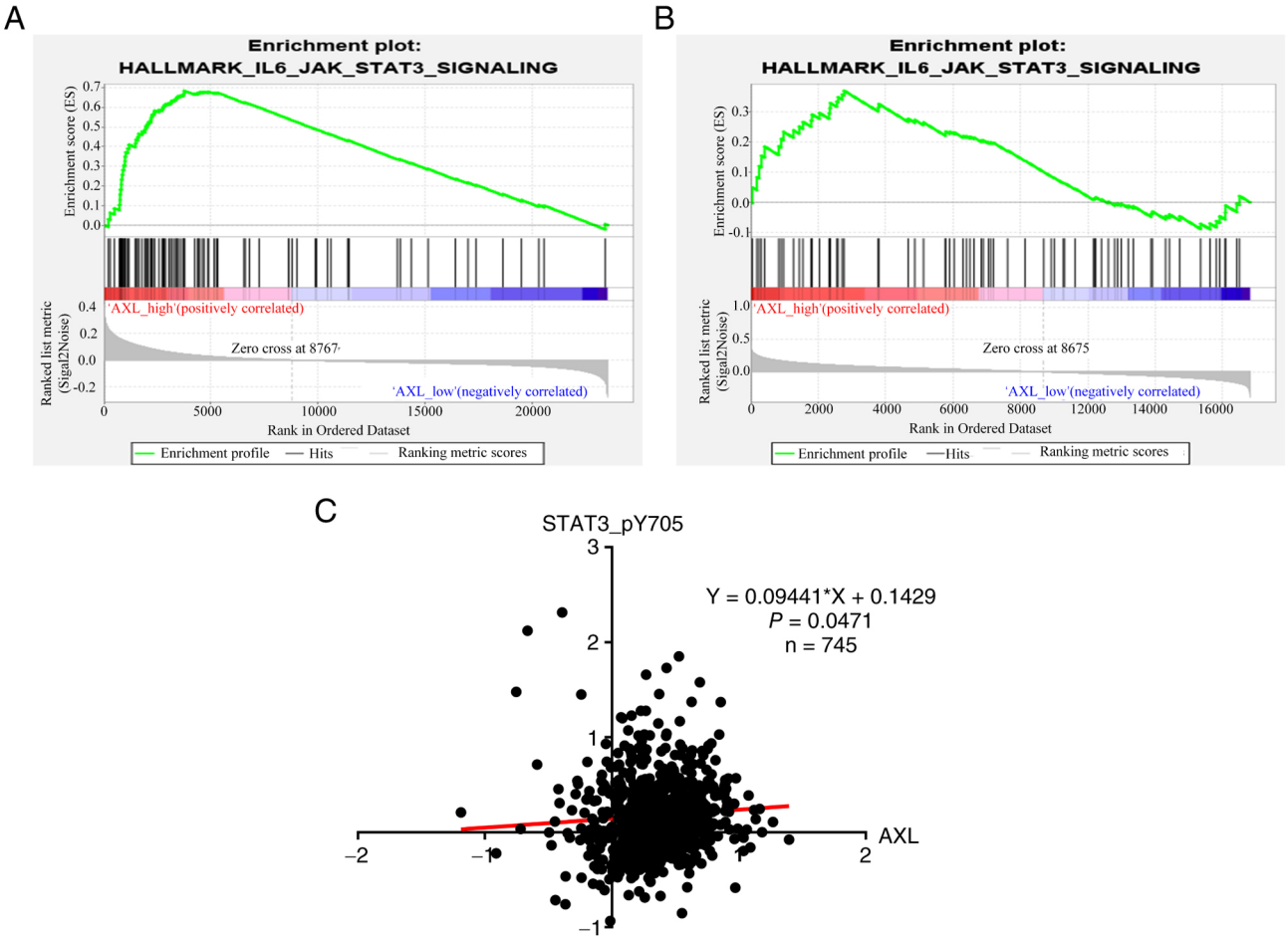

Figure 3. AXL is associated with STAT3 signaling, as revealed by the analysis of mRNA and protein data of clinical breast cancer samples. (A) Gene set enrichment analysis of GSE102484, mRNA expression data from 683 patients with invasive breast cancer; IL6_JAK_STAT3 signaling in AXL-high tumors vs. AXL-low tumors is displayed. (B) Gene set enrichment analysis of GSE9893, mRNA expression data from 155 primary breast cancers; IL6_JAK_STAT3 signaling in AXL-high tumors vs. AXL-low tumors is displayed. (C) Association of AXL and p-STAT3 (pY705) in breast invasive carcinoma; data are from The Cancer Proteome Atlas and were analyzed using Prism 8. NES, normalized enrichment score.

AXL expression correlates with STAT3 signaling in clinical BC samples. GSEA analysis of the GSE102484 and GSE9893 datasets revealed that IL6_JAK_STAT3 signaling was significantly enriched in AXL-high BC tumors compared with AXL-low tumors [normalized enrichment score (NES)=1.57, P=0.027 for GSE102484; NES=1.58, P=0.008 for GSE9893] (Fig. 3A and B). TCPA dataset analysis also revealed a positive correlation between AXL protein expression and p-STAT3 (Y705) levels (Fig. 3C). These clinical data support a close association between AXL and STAT3 activation in BC.

Discussion

The present study demonstrated that AXL was associated with STAT3 activation in BC. AXL overexpression enhanced STAT3 phosphorylation, nuclear translocation and transcriptional activity, whereas AXL knockdown or inhibition suppressed STAT3 activation. Clinical dataset analyses further validated the positive correlation between AXL and STAT3 signaling in samples from patients with BC.

AXL has been reported to promote cancer progression through multiple signaling pathways (6,7,13). The present study identified STAT3 as a novel downstream target of AXL in BC. AXL overexpression increased IL-6 secretion, which may contribute to STAT3 activation via the IL-6/JAK/STAT3 pathway. Additionally, AXL may activate STAT3 through other mechanisms, such as Src and JAK kinases, which are well-characterized upstream activators of STAT3 (32,33). Notably, AXL has been reported to activate Src in multiple cancer types (34-36). However, whether AXL directly phosphorylates STAT3 warrants further investigations.

Constitutive STAT3 activation is a key driver of BC progression, regulating cell proliferation, survival and metastasis (18,19,37). The clinical relevance of the AXL-STAT3 axis is highlighted by their positive correlation in datasets of patients with BC. AXL-high tumors exhibit enhanced STAT3 signaling, which may predict a poor prognosis and therapeutic response. Therefore, the AXL-STAT3 axis represents a potential prognostic biomarker and therapeutic target for BC, particular TNBC, which frequently exhibits the co-overexpression of AXL and STAT3 (19,37-39). From a translational perspective, the AXL-STAT3 signaling axis, as proposed in the present study, represents a subtype-specific actionable target, particularly for TNBC, which lacks effective targeted therapies. A high expression of AXL accompanied by STAT3 hyperactivation may serve as a prognostic biomarker

and predictive indicator of poor outcomes and therapeutic resistance in BC, particularly TNBC. The selective AXL inhibitor, R428 (bemcentinib), has exhibited promising anti-tumor efficacy in preclinical models (11,40-43) and under early-phase clinical trials for TNBC (NCT03184558) (14). The combined inhibition of AXL and STAT3 may further enhance therapeutic efficacy by blocking this oncogenic signaling cascade more completely, providing a novel precision strategy for TNBC and other AXL/STAT3-activated BC subtypes.

The present study has certain limitations that should be acknowledged. First, *in vivo* experiments to validate the AXL-STAT3 axis are currently lacking, which the authors plan to address in BC animal models in future research. Second, the exact mechanisms by which AXL activates STAT3 require further investigation. In particular, co-immunoprecipitation (co-IP) assays could provide direct biochemical evidence of protein-protein interaction and represent a promising approach to determine whether AXL directly activates STAT3. Finally, future studies are warranted to explore the therapeutic potential of combining AXL and STAT3 inhibition for BC treatment. In conclusion, the present study reveals that AXL is functionally associated with STAT3 activation in BC, providing novel insight into the molecular mechanisms of BC progression. Targeting the AXL-STAT3 axis may represent a promising therapeutic strategy for patients with BC.

Acknowledgements

Not applicable.

Funding

The present study was supported by Jining Key Research and Development Plan Project (grant no. 2025YXNS067).

Availability of data and materials

The data generated in the present study may be requested from the corresponding author.

Authors' contributions

HZ and QG designed the experiments. GZ, XS, JZ, ZZ, XL, FY, ZG, CG, YaH, MZ, JE, YX, JuL, YuH, XM, RY and JiL performed the experiments. GZ, XS analyzed the data and wrote the manuscript. HZ and QG confirm the authenticity of all the raw data. All authors read and approved the final version of the manuscript.

Ethics approval and consent to participate

Not applicable.

Patient consent for publication

Not applicable.

Competing interests

The authors declare that they have no competing interests.

References

1. Jemal A, Bray F, Center MM, Ferlay J, Ward E and Forman D: Global cancer statistics. CA Cancer J Clin 61: 69-90, 2011.
2. Bray F, Laversanne M, Sung H, Ferlay J, Siegel RL, Soerjomataram I and Jemal A: Global cancer statistics 2022: GLOBOCAN estimates of incidence and mortality worldwide for 36 cancers in 185 countries. CA Cancer J Clin 74: 229-263, 2024.
3. Harbeck N, Penault-Llorca F, Cortes J, Gnant M, Houssami N, Poortmans P, Ruddy K, Tsang J and Cardoso F: Breast cancer. Nat Rev Dis Primers 5: 66, 2019.
4. Kaleem M, Gangane P, Mujtaba MA, Kanekar A, Shahzad N, Alzahrani AR, Zafar A and Ahmad A: The advancements in targeted therapeutic strategies for breast cancer via intervention of natural molecules: An insight into cellular and molecular mechanisms. Pathol Res Pract 278: 156338, 2026.
5. Deeptha TC, Nabeela NK, Pushparaj C, Narayanasamy A, Manickam P, Thiruvenkataswamy S and Sennimalai R: Novel therapeutic approaches targeting cancer stem cells: Unveiling new frontiers in breast cancer treatment. Pathol Res Pract 266: 155800, 2025.
6. Tang Y, Zang H, Wen Q and Fan S: AXL in cancer: A modulator of drug resistance and therapeutic target. J Exp Clin Cancer Res 42: 148, 2023.
7. Liu Y, Xu L, Dou Y and He Y: AXL: Shapers of tumor progression and immunosuppressive microenvironments. Mol Cancer 24: 11, 2025.
8. Zhu C, Wei Y and Wei X: AXL receptor tyrosine kinase as a promising anti-cancer approach: Functions, molecular mechanisms and clinical applications. Mol Cancer 18: 153, 2019.
9. Qian C, Wang C and Liu F: AXL in cardiovascular diseases: Pathophysiological insights and clinical perspectives. Pathol Res Pract 272: 156120, 2025.
10. Gjerdrum C, Tiron C, Høiby T, Stefansson I, Haugen H, Sandal T, Collett K, Li S, McCormack E, Gjertsen BT, *et al*: Axl is an essential epithelial-to-mesenchymal transition-induced regulator of breast cancer metastasis and patient survival. Proc Natl Acad Sci USA 107: 1124-1129, 2010.
11. Ji J, Ding Y, Kong Y, Fang M, Yu X, Lai X and Gu Q: Triple-negative breast cancer cells that survive ionizing radiation exhibit an Axl-dependent aggressive radioresistant phenotype. Exp Ther Med 26: 448, 2023.
12. Chang H, An R, Li X, Lang X, Feng J and Lv M: Anti-Axl monoclonal antibodies attenuate the migration of MDA-MB-231 breast cancer cells. Oncol Lett 22: 749, 2021.
13. Zhang G, Wang M, Zhao H and Cui W: Function of Axl receptor tyrosine kinase in non-small cell lung cancer. Oncol Lett 15: 2726-2734, 2018.
14. Yadav M, Sharma A, Patne K, Tabasum S, Suryavanshi J, Rawat L, Machaalani M, Eid M, Singh RP, Choueiri TK, *et al*: AXL signaling in cancer: From molecular insights to targeted therapies. Signal Transduct Target Ther 10: 37, 2025.
15. Eriksen Gjerstad M, Aehnlich P, Gelebart P and Mc Cormack E: AXL tyrosine kinases: A growing isoform family that promotes cancer pathogenesis. Cancer Res 85: 2561-2573, 2025.
16. Johnson DE, O'Keefe RA and Grandis JR: Targeting the IL-6/JAK/STAT3 signalling axis in cancer. Nat Rev Clin Oncol 15: 234-248, 2018.
17. Zhang G, Hou S, Li S, Wang Y and Cui W: Role of STAT3 in cancer cell epithelial-mesenchymal transition (review). Int J Oncol 64: 48, 2024.
18. Ma JH, Qin L and Li X: Role of STAT3 signaling pathway in breast cancer. Cell Commun Signal 18: 33, 2020.
19. Qin JJ, Yan L, Zhang J and Zhang WD: STAT3 as a potential therapeutic target in triple negative breast cancer: A systematic review. J Exp Clin Cancer Res 38: 195, 2019.
20. Meyer AS, Miller MA, Gertler FB and Lauffenburger DA: The receptor AXL diversifies EGFR signaling and limits the response to EGFR-targeted inhibitors in triple-negative breast cancer cells. Sci Signal 6: ra66, 2013.
21. Zhang G, Kong X, Wang M, Zhao H, Han S, Hu R, Huang J and Cui W: AXL is a marker for epithelial-mesenchymal transition in esophageal squamous cell carcinoma. Oncol Lett 15: 1900-1906, 2018.
22. Khera L, Vinik Y, Maina F and Lev S: The AXL-PYK2-PKCα axis as a nexus of stemness circuits in TNBC. Life Sci Alliance 4: e202000985, 2021.
23. Kim TH, Lee D, Oh HJ, Ham IH, Tran TT, Lee Y, Kim TM, Brekken RA, Zhang Z, Ke D and Hur H: Cancer-associated fibroblast-derived GAS6 increases resistance to chemotherapy through AXL/STAT3/ABCG1 in gastric cancer. Br J Cancer 134: 72-84, 2026.

24. Hung CN, Chen M, DeArmond DT, Chiu CH, Limboy CA, Tan X, Kusi M, Chou CW, Lin LL, Zhang Z, *et al*: AXL-initiated paracrine activation of pSTAT3 enhances mesenchymal and vasculogenic supportive features of tumor-associated macrophages. Cell Rep 42: 113067, 2023.
25. Sun X, Chen H, You S, Tian Z, Wang Z, Liu F, Hu W, Zhang H, Zhang G, Zhao H and Guo Q: AXL upregulates c-Myc expression through AKT and ERK signaling pathways in breast cancers. Mol Clin Oncol 18: 22, 2023.
26. Han S, Wang Y, Ge C, Gao M, Wang X, Wang F, Sun L, Li S, Dong T, Dang Z, *et al*: Pharmaceutical inhibition of AXL suppresses tumor growth and invasion of esophageal squamous cell carcinoma. Exp Ther Med 20: 41, 2020.
27. Livak KJ and Schmittgen TD: Analysis of relative gene expression data using real-time quantitative PCR and the 2(-Delta Delta C(T)) method. Methods 25: 402-408, 2001.
28. Cheng SH, Huang TT, Cheng YH, Tan TBK, Horng CF, Wang YA, Brian NS, Shih LS and Yu BL: Validation of the 18-gene classifier as a prognostic biomarker of distant metastasis in breast cancer. PLoS One 12: e0184372, 2017.
29. Chanrion M, Negre V, Fontaine H, Salvetat N, Bibeau F, Mac Grogan G, Mauriac L, Katsaros D, Molina F, Theillet C and Darbon JM: A gene expression signature that can predict the recurrence of tamoxifen-treated primary breast cancer. Clin Cancer Res 14: 1744-1752, 2008.
30. Tang Z, Kang B, Li C, Chen T and Zhang Z: GEPIA2: An enhanced web server for large-scale expression profiling and interactive analysis. Nucleic Acids Res 47 (W1): W556-W560, 2019.
31. Su YF, Shen PC, Huang WY, Hung YJ, Huang TW, Lin CY and Shieh YS: Nuclear translocation of Axl contributes to the malignancy of oral cancer cells. J Dent Sci 19: 438-447, 2024.
32. Hu Y, Dong Z and Liu K: Unraveling the complexity of STAT3 in cancer: Molecular understanding and drug discovery. J Exp Clin Cancer Res 43: 23, 2024.
33. Kim LC, Song L and Haura EB: Src kinases as therapeutic targets for cancer. Nat Rev Clin Oncol 6: 587-595, 2009.
34. Chocarro-Calvo A, Jociles-Ortega M, García-Martinez JM, Louphrasitthiphol P, Carvalho-Marques S, Vivas-García Y, Ramírez-Sánchez A, Chauhan J, Fiuza MC, Duran M, *et al*: Fatty acid uptake activates an AXL-CAV1-β-catenin axis to drive melanoma progression. Genes Dev 39: 463-489, 2025.
35. Dong M, Xiao Q, Hu J, Cheng F, Zhang P, Zong W, Tang Q, Li X, Mao F, He Y, *et al*: Targeting LRIG2 overcomes resistance to EGFR inhibitor in glioblastoma by modulating GAS6/AXL/SRC signaling. Cancer Gene Ther 27: 878-897, 2020.
36. Xiao Y, Zhao H, Tian L, Nolley R, Diep AN, Ernst A, Fuh KC, Miao YR, von Eyben R, Leppert JT, *et al*: S100A10 is a critical mediator of GAS6/AXL-induced angiogenesis in renal cell carcinoma. Cancer Res 79: 5758-5768, 2019.
37. Banerjee K and Resat H: Constitutive activation of STAT3 in breast cancer cells: A review. Int J Cancer 138: 2570-2578, 2016.
38. Ozyurt R and Ozpolat B: Therapeutic landscape of AXL receptor kinase in triple-negative breast cancer. Mol Cancer Ther 22: 818-832, 2023.
39. Khera L and Lev S: Accelerating AXL targeting for TNBC therapy. Int J Biochem Cell Biol 139: 106057, 2021.
40. Zajac O, Leclere R, Nicolas A, Meseure D, Marchiò C, Vincent-Salomon A, Roman-Roman S, Schoumacher M and Dubois T: AXL controls directed migration of mesenchymal triple-negative breast cancer cells. Cells 9: 247, 2020.
41. Holland SJ, Pan A, Franci C, Hu Y, Chang B, Li W, Duan M, Torneros A, Yu J, Heckrodt TJ, *et al*: R428, a selective small molecule inhibitor of Axl kinase, blocks tumor spread and prolongs survival in models of metastatic breast cancer. Cancer Res 70: 1544-1554, 2010.
42. Loges S, Heuser M, Chromik J, Sutamtewagul G, Kapp-Schwoerer S, Crugnola M, Di Renzo N, Lemoli R, Mattei D, Fiedler W, *et al*: Bemcentinib as monotherapy and in combination with low-dose cytarabine in acute myeloid leukemia patients unfit for intensive chemotherapy: A phase 1b/2a trial. Nat Commun 16: 2846, 2025.
43. Li H, Liu Z, Liu L, Zhang H, Han C, Girard L, Park H, Zhang A, Dong C, Ye J, *et al*: AXL targeting restores PD-1 blockade sensitivity of STK11/LKB1 mutant NSCLC through expansion of TCF1^{+} CD8 T cells. Cell Rep Med 3: 100554, 2022.